

SPH Closure Submodels

(ii) For Water, we have a choice of 3 options: 2 different equations of state and 1 methodological.

(a) Tait's equation of state is

$$p = \frac{c_o^2 \rho_w}{\gamma} \left(\left(\frac{\rho}{\rho_w} \right)^\gamma - 1 \right)$$

$$\text{EoS } P = f(\rho)$$

weakly compressible

$\rho_w = 1000 \text{ kg/m}^3$ density of water, $\gamma = 7$ polytropic index, c_o is the speed of sound for $\rho = \rho_{w, k}$

Note speed of sound for each particle

$$c_i = \sqrt{\frac{\partial P}{\partial \rho}}$$

$$\frac{\partial P}{\partial \rho}$$

81

SPH Closure Submodels

This is a 'stiff' equation of state (due to $\gamma = 7$) so that density variations stay small – density variations are on the order of the Mach number squared

$$O(M^2) = O\left(\frac{v_{max}}{c_0}\right)^2$$

$$\left(0, 1 = \frac{1}{10}\right)^2 = \frac{1}{100} = 0, 1 = 1\%$$

We choose c_0 so that the Mach number $M = v_{max}/c_0 \approx 0.1$, hence **density variations are less than 1%**. This keeps the water more or less incompressible but small variations in density can lead to large pressure fluctuations

So, for this system of equations we must solve only

- (i) continuity equation
- (ii) momentum equation

- SPH uses a reduced speed of sound (not the physical exact speed of sound)

SPH Closure Submodels

(b) Morris's equation of state is ($\gamma = 1$)

$$\text{EoS : } P = f(\rho)$$

$$p = c_o^2 (\rho - \rho_w)$$

$\rho_w = 1000 \text{ kg/m}^3$ density of water, c_o is the speed of sound for $\rho = \rho_w$.

This equation has smaller pressure fluctuations, but the water is **more compressible**.

For this system of equations we must solve only

- (i) continuity equation
(ii) momentum equation

83

SPH Closure Submodels

(c) Enforce incompressibility via the pressure Poisson equation

$$\text{EoS : } P = f(\rho)$$

$$\nabla^2 p = ??$$

I put ?? Since there are various different forms of this Poisson equation

$$\left\{ \begin{array}{l} \frac{\partial p}{\partial t} = 0 \\ i.e. p = \text{const} \end{array} \right.$$

ISPH = incompressible SPH

84

Key Components for simulations using SPH

Closure Submodel 2: Viscosity

85

SPH VISCOSITY

Viscous effects can be included in 3 ways:

- (i) Artificial viscosity
- (ii) Laminar viscosity
- (iii) Turbulence models

We will look at these 3 in turn

(i) Artificial viscosity

As the name suggests, this is artificial and uses empirical coefficients to model the energy dissipation. The momentum conservation equation becomes:

In SPH notation, the momentum equation is written as

$$\frac{d \mathbf{v}_a}{dt} = - \sum_b m_b \left(\frac{P_b}{\rho_b^2} + \frac{P_a}{\rho_a^2} + \Pi_{ab} \right) \nabla_a W_{ab} + \mathbf{g}$$

86

SPH VISCOSITY

Goal is to get numerical stability

The artificial viscosity proposed by Monaghan (1992) has been used very often due to its simplicity. In the limit Π_{ij} , the viscosity term tends to the differential

$$\Pi_{ab} = \begin{cases} -\frac{\alpha \bar{c}_{ab} \mu_{ab}}{\rho_{ab}} & \mathbf{v}_{ab} \cdot \mathbf{r}_{ab} < 0 \\ 0 & \mathbf{v}_{ab} \cdot \mathbf{r}_{ab} > 0 \end{cases}$$

$$\mu_{ab} = \frac{h \mathbf{v}_{ab} \cdot \mathbf{r}_{ab}}{\mathbf{r}_{ab}^2 + \eta^2}$$

$$\mathbf{r}_{ab} = \mathbf{r}_a - \mathbf{r}_b$$

$$\mathbf{v}_{ab} = \mathbf{v}_a - \mathbf{v}_b$$

$$\bar{c}_{ab} = \frac{c_a + c_b}{2}$$

$$\eta^2 = 0.01h^2,$$

a is a free parameter that can be changed according to each problem.

Therefore it's empirical!! Yuk!

87

Riemann/Jedrzejewski
SPH

SPH VISCOSITY

(ii) Laminar viscosity

The momentum conservation equation with laminar viscous stresses is given by

$$\frac{D\mathbf{v}}{Dt} = -\frac{1}{\rho} \nabla P + \mathbf{g} + \nu_0 \nabla^2 \mathbf{v}$$

laminar flow

We cannot use a 2nd-order derivative of W for the 2nd-order viscous term as this leads to unstable simulations, so in SPH we combine two 1st-order derivatives.

Hence, the laminar stress term simplifies (Morris et al., 1997) to

$$(\nu_0 \nabla^2 \mathbf{v})_a = \sum_b m_b \left(\frac{4\nu_0 \mathbf{r}_{ab} \nabla_a W_{ab}}{(\rho_a + \rho_b) |\mathbf{r}_{ab}|^2} \right) \mathbf{v}_{ab}$$

where ν_0 is the kinetic viscosity of laminar flow.

So, in SPH notation, the momentum equation becomes:

$$\frac{d\mathbf{v}_a}{dt} = - \sum_b m_b \left(\frac{P_b}{\rho_b^2} + \frac{P_a}{\rho_a^2} \right) \nabla_a W_{ab} + \mathbf{g} + \sum_b m_b \left(\frac{4\nu_0 \mathbf{r}_{ab} \nabla_a W_{ab}}{(\rho_a + \rho_b) |\mathbf{r}_{ab}|^2} \right) \mathbf{v}_{ab}$$

88

SPH VISCOSITY: Turbulence

(iii) Turbulence Modelling

This is **specialised** and really depends on what physics you are modelling and what level of sophistication you would want in your turbulence model.

Here we just give the governing equations we are solving and the corresponding SPH equations

$$\frac{d\mathbf{v}}{dt} = -\frac{1}{\rho}\nabla P + \mathbf{g} + v_0\nabla^2\mathbf{v} + \frac{1}{\rho}\nabla\tau$$

= SPH not yet ready
for proper turbulence

τ represents the shear stresses due to turbulence.

The SPH form:

$$\begin{aligned} \frac{d\mathbf{v}_a}{dt} &= -\sum_b m_b \left(\frac{P_b}{\rho_b^2} + \frac{P_a}{\rho_a^2} \right) \nabla_a W_{ab} + \mathbf{g} \\ &+ \sum_b m_b \left(\frac{4v_0 \mathbf{r}_{ab} \nabla_a W_{ab}}{(\rho_a + \rho_b) |\mathbf{r}_{ab}|^2} \right) \mathbf{v}_{ab} + \sum_b m_b \left(\frac{\tau_b}{\rho_b^2} + \frac{\tau_a}{\rho_a^2} \right) \nabla_a W_{ab} \end{aligned}$$

Laminar Turbulent

89

SPH VISCOSITY: Turbulence

For the turbulent stresses we can choose a number of different options

- (i) Simple mixing length models
- (ii) RANS models
- (iii) Large Eddy Simulation (LES) simulations

The interested reader is referred to Violeau & Issa (2004) for a review of turbulence models for SPH.

Turbulence in SPH is a difficult subject since the particles are moving themselves - there is not the huge quantity of knowledge about Lagrangian turbulent statistics that exists for the Eulerian frame of reference.

Moreover, the particles may not follow the correct particle paths depending on the accuracy of the simulation so the shear may not be accurately described. Hence, the description of the Lagrangian turbulence is still very under-developed.

90

Key Components for simulations using SPH

Boundary Conditions: a brief overview

91

SPH BOUNDARY CONDITIONS

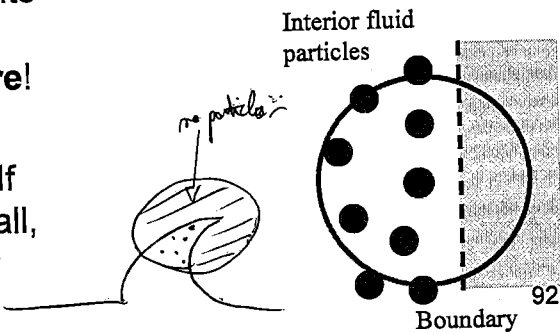
Now, let's discuss boundaries in SPH.

When SPH was developed over 30 years ago, the technique was designed for **astrophysics simulating galaxy formation, etc.**

Up there (in space) **there are no boundaries!!** They didn't need to consider boundary conditions, but for engineering, all our simulations will have boundaries either **open or closed (solid wall).**

The immediate problem that presents itself is the old problem with the kernel- **there are no particles there!**

A more philosophical Question is: If there are no fluid particles in the wall, **what role or function should any artificial particles take?**

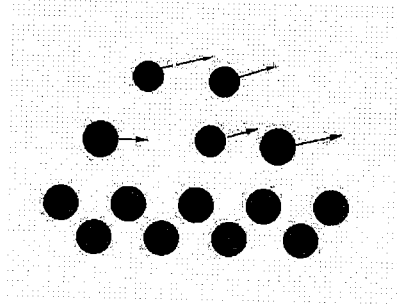


Solid Wall Boundary Conditions

There are 4 basic choices:

- (i) Fluid Particles do not move & remain still.

We calculate $\frac{d\rho}{dt}$, $\frac{de}{dt}$ but $v = 0$ for all boundary particles



Advantages:

Simple

Disadvantages:

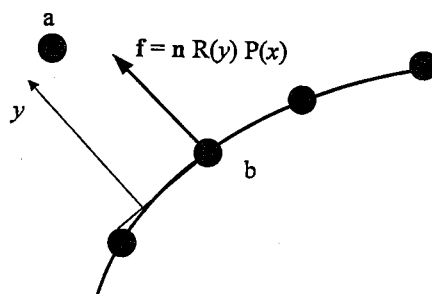
{ Produces a very large Boundary Layer!
Particles penetrate the wall

93

Solid Wall Boundary Conditions

- (ii) Repulsive Force

This can take various forms such as Lennard-Jones forces or an empirical function with a singularity so that the force increases as the particle nears the boundary



- Repulsive force calculation
- $R(y)$ is infinite as $y \rightarrow 0$

\therefore = introduce non physical force
= don't use it"

Advantages:

Simple

Virtually avoids wall penetration

Disadvantages:

{ Empirical!

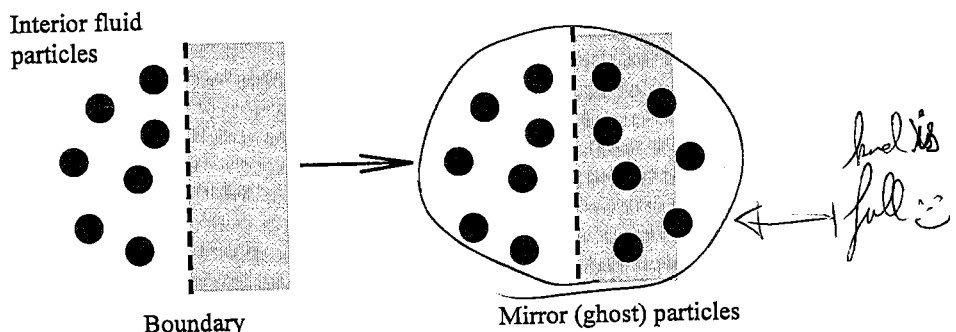
{ Does not complete support of the kernel for WPs

94

Solid Wall Boundary Conditions

(iii) Mirror Particles

Actual particles inside the computational domain are reflected to create Mirror Images



Advantages:

Intuitive approach (like potential flow methods)

Particles cannot penetrate since they would cross through themselves!

Disadvantages:

- Extremely difficult for any geometry other than a straight wall
- Corners (and therefore vorticity) very difficult to get right



lack of symmetry

Solid Wall Boundary Conditions

(iv) Using Gauss' Theorem for the surface integration.

We Recall the basic SPH *continuous* interpolation from which we derive the discrete form:

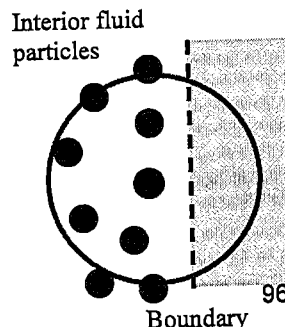
$$\langle A(\mathbf{r}) \rangle = \int_{\Omega} A(\mathbf{r}') W(\mathbf{r} - \mathbf{r}', h) d\Omega$$

We are predominantly interested in gradients:

$$\langle \nabla A(\mathbf{r}) \rangle = \int_{\Omega} A(\mathbf{r}') \nabla W(\mathbf{r} - \mathbf{r}', h) d\Omega$$

In the vicinity of the boundary, the kernel will extend beyond the computational domain

The partition of unity property is no longer satisfied → inaccuracy



Solid Wall Boundary Conditions

Hence, a number of people have tried splitting the derivative approximation into two parts

$$\begin{aligned}\langle \nabla A(\mathbf{r}) \rangle &= \int_{\Omega} A(\mathbf{r}') \nabla W(\mathbf{r} - \mathbf{r}', h) d\Omega \\ &= \int_{\Omega_{\text{int}}} A(\mathbf{r}') \nabla W(\mathbf{r} - \mathbf{r}', h) d\Omega + \int_{\Omega_{\text{bou}}} A(\mathbf{r}') \nabla W(\mathbf{r} - \mathbf{r}', h) d\Omega\end{aligned}$$

The **big difficulty** with this is that we cannot evaluate the second term without one of the previous approaches.

However, we can apply **Gauss' theorem** to the second term to turn this into a surface integral over the boundary

$$\langle \nabla A(\mathbf{r}) \rangle = \int_{\Omega_{\text{int}}} A(\mathbf{r}') \nabla W(\mathbf{r} - \mathbf{r}', h) d\Omega + \int_{S_{\text{bou}}} A(\mathbf{r}') W(\mathbf{r} - \mathbf{r}', h) dS$$

Advantages:	Theoretically correct
Disadvantages:	Very difficult to discretise in a consistent way ⁹⁷

Solid Wall Boundary Conditions

(v) **Transpose fluid particles to an Eulerian domain**, apply method of characteristics and transpose back again (Marongiu et al. 2007)

(vi) **Mixture of above approaches**

Numerous combinations of the above approaches have been tried

There is no general agreement on the best BC, each SPH practitioner chooses the most suitable BC for the problem.

Open Boundaries

These are very difficult and have been attempted to limited extent (Tafuni et al. 2018).

SPH Time Integration

Let's see how we can march the simulation through time.

There is an enormous body of work on time stepping. We have a huge choice of schemes (some more sophisticated than others). As our particles (computation or nodal points) are moving, we must use at least a scheme that is **2nd-order accurate in time**.

To begin with we rewrite all our governing equations in the following simplified form:

$$\left\{ \begin{array}{ll} \frac{dv_a}{dt} = F_a & \text{Momentum} \\ \frac{d\rho_a}{dt} = D_a & \text{Continuity} \\ \frac{dr_a}{dt} = v_a & \text{Position} \\ \frac{de_a}{dt} = E_a & \text{Energy} \end{array} \right.$$

A quick recap on notations for time stepping:

v_a^n ← Superscript n means time level n
 a ← Subscript a means particle a

such that time is given by $t = \sum_1^n \Delta t = n \Delta t$
(for constant Δt)

SPH Time Integration

(i) 2nd-order accurate Predictor-Corrector

Predictor step: This scheme predicts the evolution in time as

$$\frac{v_a^{n+1} - v_a^n}{\frac{\Delta t}{2}} = F_a^n = \frac{dv_a}{dt}$$

$$\left\{ \begin{array}{l} v_a^{n+1/2} = v_a^n + \frac{\Delta t}{2} F_a^n ; \rho_a^{n+1/2} = \rho_a^n + \frac{\Delta t}{2} D_a^n \\ r_a^{n+1/2} = r_a^n + \frac{\Delta t}{2} v_a^n ; e_a^{n+1/2} = e_a^n + \frac{\Delta t}{2} E_a^n \end{array} \right.$$

$$D_a = \frac{d\rho_a}{dt}$$

Corrector step: These values are then corrected using forces at half step

$$\left\{ \begin{array}{l} v_a^{n+1/2} = v_a^n + \frac{\Delta t}{2} F_a^{n+1/2} \\ r_a^{n+1/2} = r_a^n + \frac{\Delta t}{2} v_a^{n+1/2} \end{array} \right. \quad \begin{array}{l} \rho_a^{n+1/2} = \rho_a^n + \frac{\Delta t}{2} D_a^{n+1/2} \\ e_a^{n+1/2} = e_a^n + \frac{\Delta t}{2} E_a^{n+1/2} \end{array}$$

Finally, the values are calculated at the end of the time step

$$\left\{ \begin{array}{l} v_a^{n+1} = 2v_a^{n+1/2} - v_a^n \\ r_a^{n+1} = 2r_a^{n+1/2} - r_a^n \end{array} \right. \quad \begin{array}{l} \rho_a^{n+1} = 2\rho_a^{n+1/2} - \rho_a^n \\ e_a^{n+1} = 2e_a^{n+1/2} - e_a^n \end{array}$$

SPH Time Integration

(ii) Velocity Verlet (from Molecular Dynamics) \rightarrow DSPH

This time stepping algorithm is split into two parts:

In general, variables are calculated according to

$$\left\{ \begin{array}{l} v_a^{n+1} = v_a^n + 2\Delta t F_a^n \\ r_a^{n+1} = r_a^n + \Delta t v_a^n + 0.5\Delta t^2 F_a^n \\ \rho_a^{n+1} = \rho_a^n + 2\Delta t D_a^n \\ e_a^{n+1} = e_a^n + 2\Delta t E_a^n \end{array} \right.$$

except for position

\Rightarrow Velocity & position are decoupled

~~needs~~ Once every M time steps (M on the order of 50 time steps), variables are calculated according to

$$\left\{ \begin{array}{l} v_a^{n+1} = v_a^n + \Delta t F_a^n \\ r_a^{n+1} = r_a^n + \Delta t v_a^n + 0.5\Delta t^2 F_a^n \\ \rho_a^{n+1} = \rho_a^n + \Delta t D_a^n \\ e_a^{n+1} = e_a^n + \Delta t E_a^n \end{array} \right.$$

This is to stop the time integration diverging since the equations are no longer coupled.

101

SPH Time Integration

(iii) Leap-Frog Scheme

This follows the standard formula

$$\left\{ \begin{array}{l} v_a^{n+1/2} = v_a^{n-1/2} + \frac{1}{2}(\Delta t^n + \Delta t^{n-1}) F_a^n \\ r_a^{n+1} = r_a^n + \Delta t v_a^{n+1/2} \\ v_a^n = \frac{1}{2}(v_a^{n+1/2} + v_a^{n-1/2}) \\ \rho_a^{n+1} = \rho_a^n (1 - D_a^n \Delta t^n) \\ e_a^{n+1/2} = e_a^n + \frac{\Delta t}{2} E_a^n \end{array} \right.$$

except position

(iv) Symplectic or Geometric Integrators

(DSPH)

These we will not cover here, but they are time reversible and hence have the potential to be very important!

102

SPH Variable Time Step

Just as for many numerical simulations, we cannot take too big a timestep. If we do, the simulations become unstable!

Like all other CFD schemes, we use a timestep based on the **CFL condition** which dictates the maximum timestep allowable, e.g.

$$\Delta t = CFL \frac{\Delta x}{U_{\max}}$$

$CFL < 1$

However, if there is not much going on in our computational domain, we can **vary or change our timestep** and then make it smaller when we need to according to some criteria.

103

SPH Variable Time Step

Time-step control is dependant on the **CFL condition**, the forcing terms and the viscous diffusion term (Monaghan; 1989). A variable time step Δt is calculated according to Monaghan and Kos (1999):

$$\Delta t_f = \min_a \left(\sqrt{h/|f_a|} \right)$$

Timestep based on force

$$\Delta t_{cv} = \min_a \frac{h}{c_s + \max_b \left| \frac{h \mathbf{v}_{ab} \cdot \mathbf{r}_{ab}}{\mathbf{r}_{ab}^2} \right|}$$

Time step based on velocity

c ↑ then Δt ↓

$$\Delta t = 0.3 \cdot \min(\Delta t_f, \Delta t_{cv})$$

Choice of smallest with CFL number of 0.3

Here Δt_f is based on the force per unit mass $|f_a|$, and Δt_{cv} combines the Courant and the viscous time-step controls

104

SPH DENSITY ISSUES

Despite all the best efforts of the formulation, as indicated in the discussion of SPH accuracy, there are some quite severe issues. This is particularly the case with density.

Why? With the classical formulation, it depends on the equation of state.

Let's consider water which uses the Tait equation of state: EoS

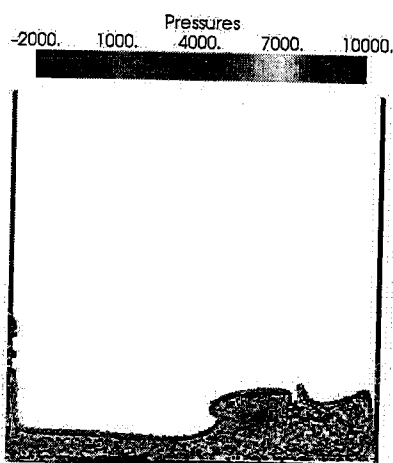
$$p = \frac{c_o^2 \rho_w}{\gamma} \left(\left(\frac{\rho}{\rho_w} \right)^\gamma - 1 \right)$$

remember that $\rho_w = 1000 \text{ kg/m}^3$ density of water, $\gamma = 7$ polytropic index, c_o is the speed of sound for $\rho = \rho_w$.

105

SPH DENSITY ISSUES

Well what happens? Here we see the pressure field for a 2-D Dam break simulation. The pressure is very noisy!!!!



The problem is very clear. The methods gets the **kinematics correct**, but not the dynamics. In this case, very small density variations give us enormous pressure variations ~~which~~ are not physical.

which

Small $\Delta\rho$ gives large ΔP : \rightarrow density filtering

106

SPH DENSITY ISSUES

So, what can we do?

We have several different options:

- (i) Use a different formulation (not covered here)
- (ii) Density filtering

We will look at Option (ii) because it is well tested. For density filtering, we essentially re-initialise the density **every 50 timesteps** using either a zeroth-order or first order correction

107

SPH DENSITY FILTERING

(i) Zeroth Order – Shepard Filter

The Shepard filter is a quick and simple correction to the density field, and the following procedure is applied every 30 time steps

$$\rho_a^{new} = \sum_b \rho_b \tilde{W}_{ab} \cdot \frac{m_b}{\rho_b} = \sum_b m_b \tilde{W}_{ab}$$

where the kernel has been corrected using a zeroth-order correction

$$\tilde{W}_{ab} = \frac{W_{ab}}{\sum_b W_{ab} \frac{m_b}{\rho_b}}$$

108

SPH DENSITY FILTERING

(ii) First Order – Moving Least Squares (MLS)

The Moving Least Squares (MLS) is a first-order correction so that the linear variation of the density field can be exactly reproduced

$$\rho_a^{new} = \sum_b \rho_b W_{ab}^{MLS} \frac{m_b}{\rho_b} = \sum_b m_b W_{ab}^{MLS}$$

The corrected kernel is evaluated as follows:

$$W_{ab}^{MLS} = W_b^{MLS}(\mathbf{r}_a) = \beta(\mathbf{r}_a) \cdot (\mathbf{r}_a - \mathbf{r}_b) W_{ab}$$

$$\text{In 2-D: } W_{ab}^{MLS} = [\beta_0(\mathbf{r}_a) + \beta_{1x}(\mathbf{r}_a)(x_a - x_b) + \beta_{1z}(\mathbf{r}_a)(z_a - z_b)] W_{ab}$$

Remember for density filtering, we **re-initialise the density every 50 timesteps**, hence after 50 timesteps, we perform the above summations and the densities are given new values before the next timestep

SPH DENSITY FILTERING

where the correction vector β is given by

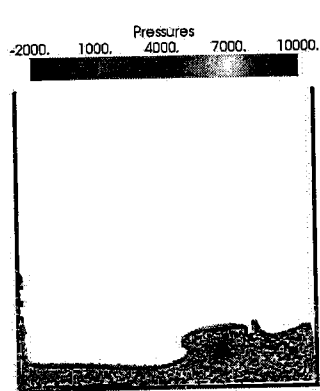
$$\beta(\mathbf{r}_a) = \begin{bmatrix} \beta_0 \\ \beta_{1x} \\ \beta_{1z} \end{bmatrix} = \mathbf{A}^{-1} \begin{bmatrix} 1 \\ 0 \\ 0 \end{bmatrix} \quad \mathbf{A} = \sum_b W_b(\mathbf{r}_a) \tilde{\mathbf{A}} V_b$$

with the matrix being given by

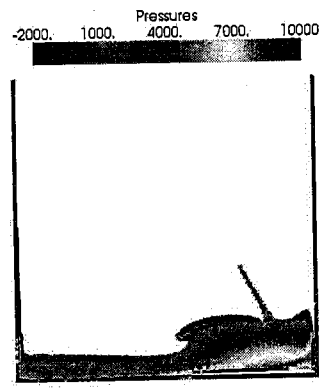
$$\tilde{\mathbf{A}} = \begin{bmatrix} 1 & (x_a - x_b) & (z_a - z_b) \\ (x_a - x_b) & (x_a - x_b)^2 & (z_a - z_b)(x_a - x_b) \\ (z_a - z_b) & (x_a - x_b)(z_a - z_b) & (z_a - z_b)^2 \end{bmatrix}$$

SPH DENSITY FILTERING

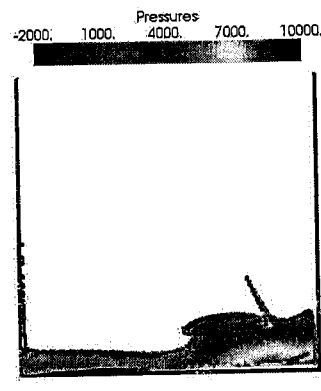
So, what improvement does this give? Well let's compare:



Artificial Viscosity



Artificial Viscosity
with Shepard Filter



Artificial Viscosity
with MLS Filter

So, you can see that just a simple density filter cleans up the results, making the final results more 'believable' (but not properly validated)

111

A numerical scheme with better
pressure field

δ -SPH

Molteni & Colagrossi (2009)

112

Standard SPH formulation

113

Continuity equation: $\frac{d\rho_a}{dt} = \sum_b m_b (\mathbf{v}_a - \mathbf{v}_b) \cdot \nabla W_{ab}$

Momentum equation: $\frac{d\mathbf{v}_a}{dt} = - \sum_b m_b \left(\frac{P_b}{\rho_b^2} + \frac{P_a}{\rho_a^2} + \Pi_{ab} \right) \nabla_a W_{ab} + \mathbf{g}$

Lagrangian motion: $\frac{d\mathbf{x}_a}{dt} = \mathbf{v}_a$

Equation of state: $P_a = f(\rho_a)$

- ✓ Conservation of mass
- ✓ Conservation of linear and angular momenta
- ✓ Conservation of (kinetic + potential + internal) energy (if no dissipation in the momentum equation)

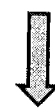
Standard SPH formulation

Generally....

- the SPH simulation is initialized by imposing a uniform particle distribution
(or, at least, as regular as possible!)
=> the volumes are initially uniform
- the density field is assigned as an initial condition
(and generally it is not constant all over the fluid domain)
=> the particles may have different masses

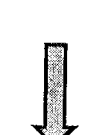
$$\frac{d\mathbf{m}_a}{dt} = 0$$

$$V_i = V_0 \quad \forall i$$



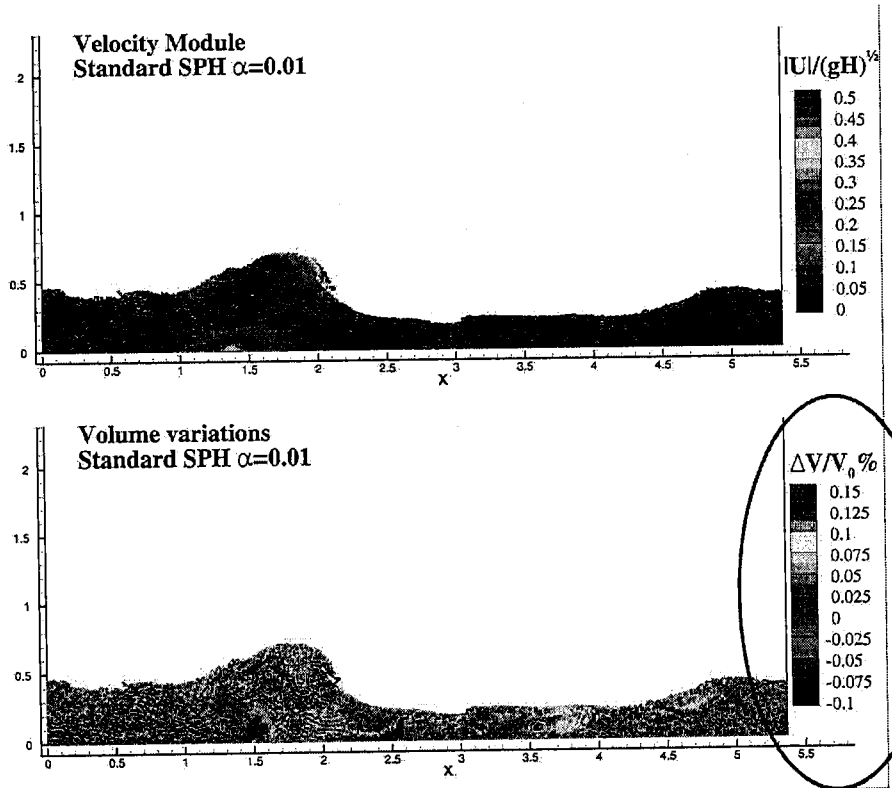
$$t = t_0: m_i = \rho_i V_0$$

- During the simulation, the masses do not change while the density field evolves according to the physical equations



$$V_i = \frac{m_i}{\rho_i}$$

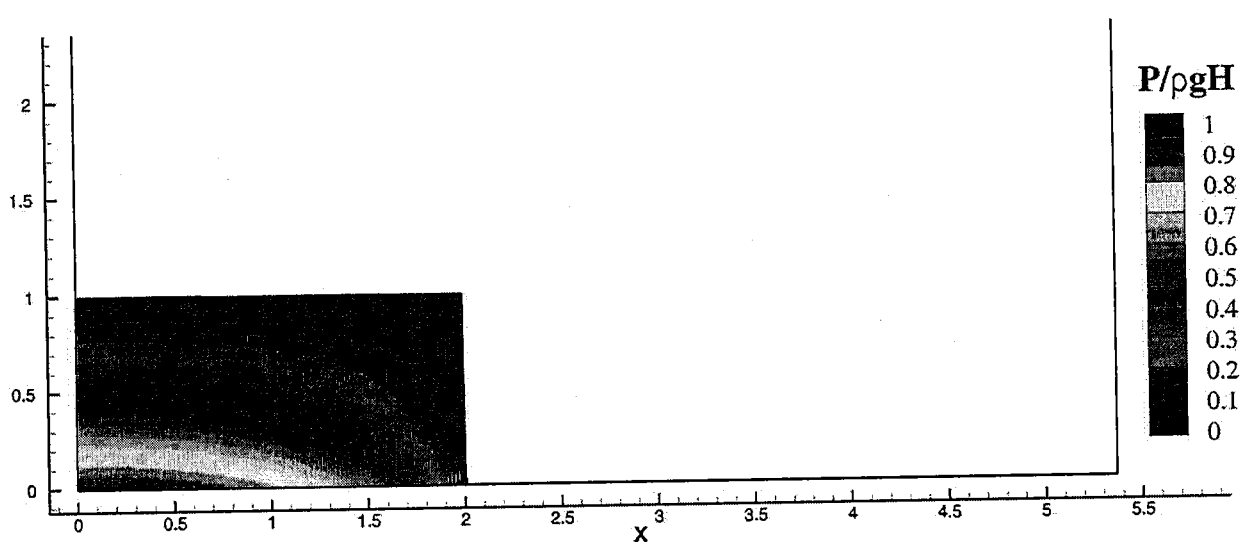
Standard SPH formulation



Standard SPH formulation

Generally, the velocity field and particle positions are good....

What about other relevant quantities like pressure?



Dam-break flow: "inviscid fluid" simulated with artificial viscosity ($\alpha=0.01$)

Standard SPH formulation

PROS:

- ✓ explicit scheme => good for parallelization (e.g. 3D simulations)
- ✓ Implicit fulfilment of the free-surface boundary conditions
 - => good for simulations with complex interface deformations/fragmentations

CONS:

- large sound speed => small time step
- weakly-compressible fluid => acoustic noise
- central-explicit scheme (+ nonlinearities) => spurious numerical noise

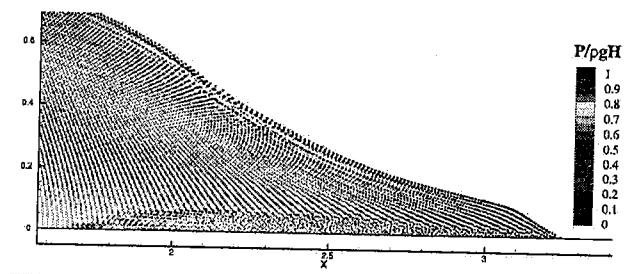
numerical schemes to reduce/avoid the spurious numerical noise

Standard SPH formulation

Kinematics is correct, but pressure field is noisy!

Main sources of noise on the pressure field:

- Numerical scheme: centred + explicit
- Physical model: acoustic waves
- Lagrangian character:
particle resettlement

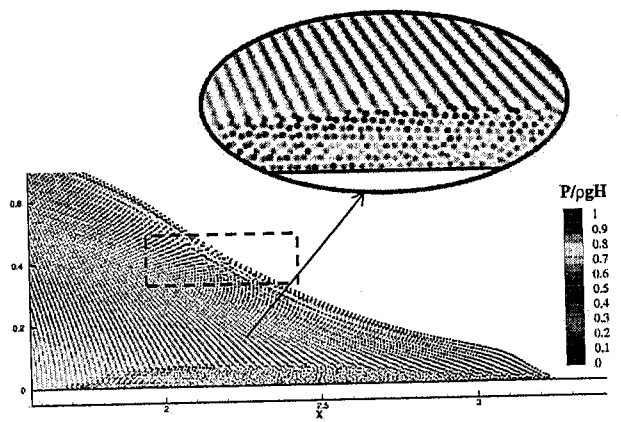


Standard SPH formulation

Kinematics is correct, but pressure field is noisy!

Main sources of noise on the pressure field:

- Numerical scheme: centred + explicit
- Physical model: acoustic waves
- Lagrangian character:
particle resettlement



δ - SPH formulation

$$\frac{d\rho_a}{dt} = \sum_b m_b (\mathbf{v}_a - \mathbf{v}_b) \cdot \nabla W_{ab} + \boxed{\delta h c_0 \mathcal{D}_a}$$

$$\frac{d\mathbf{v}_a}{dt} = - \sum_b m_b \left(\frac{P_b}{\rho_b^2} + \frac{P_a}{\rho_a^2} + \Pi_{ab} \right) \nabla_a W_{ab} + \mathbf{g}$$

$$\frac{d\mathbf{x}_a}{dt} = \mathbf{v}_a$$

$$\mathcal{D}_a = 2 \sum_b \psi_{ab} \cdot \nabla W_{ab} V_b \quad V_b = m_b / \rho_b$$

δ is a dimensionless parameter

ψ_{ab} depends on the specific diffusive scheme adopted (see later)

δ - SPH formulation

The vector $\psi_{i,j}$ has to be **symmetric**, that is

$$\psi_{ab} = \psi_{ba} \quad \longrightarrow \quad \sum_b D_b V_b = 0$$

This ensures the consistency of the integral form of the continuity equation
(e.g. consistency with the equation of mass conservation)

with diffusion	without diffusion
$\sum_a \left[\frac{d\rho_a}{dt} - \sum_b m_b (\mathbf{v}_a - \mathbf{v}_b) \cdot \nabla W_{ab} - \delta h c_0 D_a \right] = \sum_a \left[\frac{d\rho_a}{dt} - \sum_b m_b (\mathbf{v}_a - \mathbf{v}_b) \cdot \nabla W_{ab} \right]$	

δ - SPH formulation

$\psi_{ab} = (\rho_b - \rho_a) \frac{(\mathbf{r}_b - \mathbf{r}_a)}{\ \mathbf{r}_b - \mathbf{r}_a\ ^2}$	Molteni & Colagrossi (2009)	}
$\psi_{ab} = (\rho_b - \rho_a) \frac{(\mathbf{r}_b - \mathbf{r}_a)}{2h\ \mathbf{r}_b - \mathbf{r}_a\ }$	Ferrari et al. (2009)	

$$D_a \simeq \nabla^2 \rho_a$$

but they are inconsistent close to the free surface (**no hydrostatic solution!**)

δ - SPH formulation

To avoid such an inconsistency, Antuono et al. (2010) defined the following form:

$$\psi_{ab} = \left[(\rho_b - \rho_a) - \frac{1}{2} (\langle \nabla \rho_b \rangle^L + \langle \nabla \rho_a \rangle^L) \cdot (\mathbf{r}_b - \mathbf{r}_a) \right] \frac{(\mathbf{r}_b - \mathbf{r}_a)}{\|\mathbf{r}_b - \mathbf{r}_a\|^2}$$

- this formulation is consistent close to the free surface
- the diffusive term converges to zero if h goes to zero

Inside the fluid domain

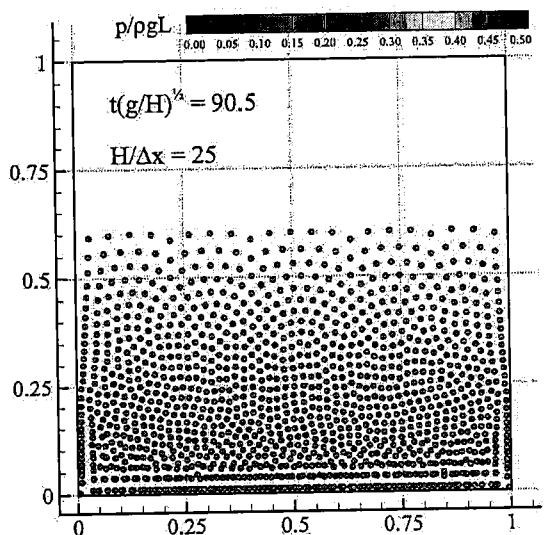
$$\mathcal{D}_i \approx \frac{h^2}{12} B_{jklq} \left(\frac{\partial^4 \rho_i}{\partial x_j \partial x_k \partial x_p \partial x_q} \right)$$

The latter scheme is called
 δ -SPH scheme

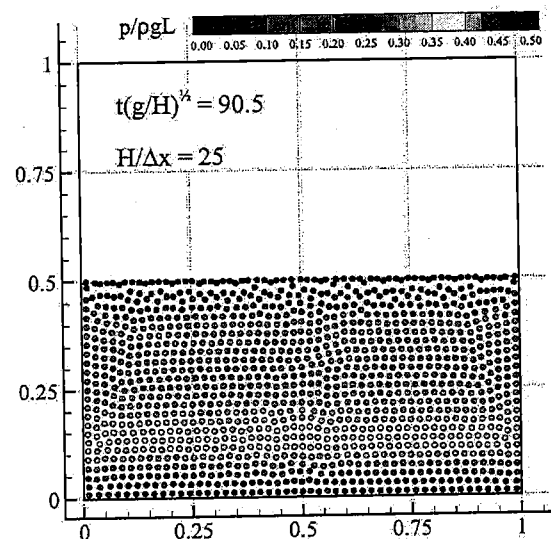
δ - SPH formulation

Hydrostatic test

Molteni & Colagrossi (2009)

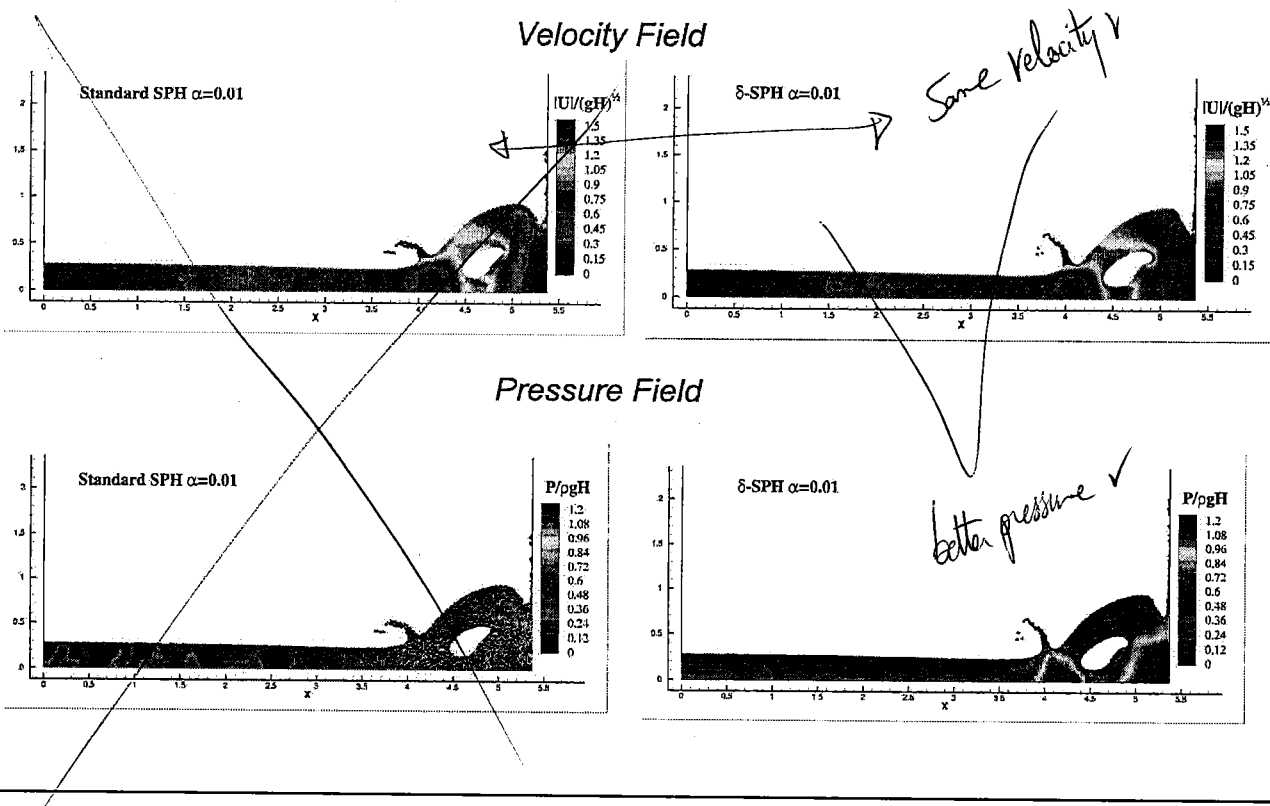


Antuono et al. (2010)

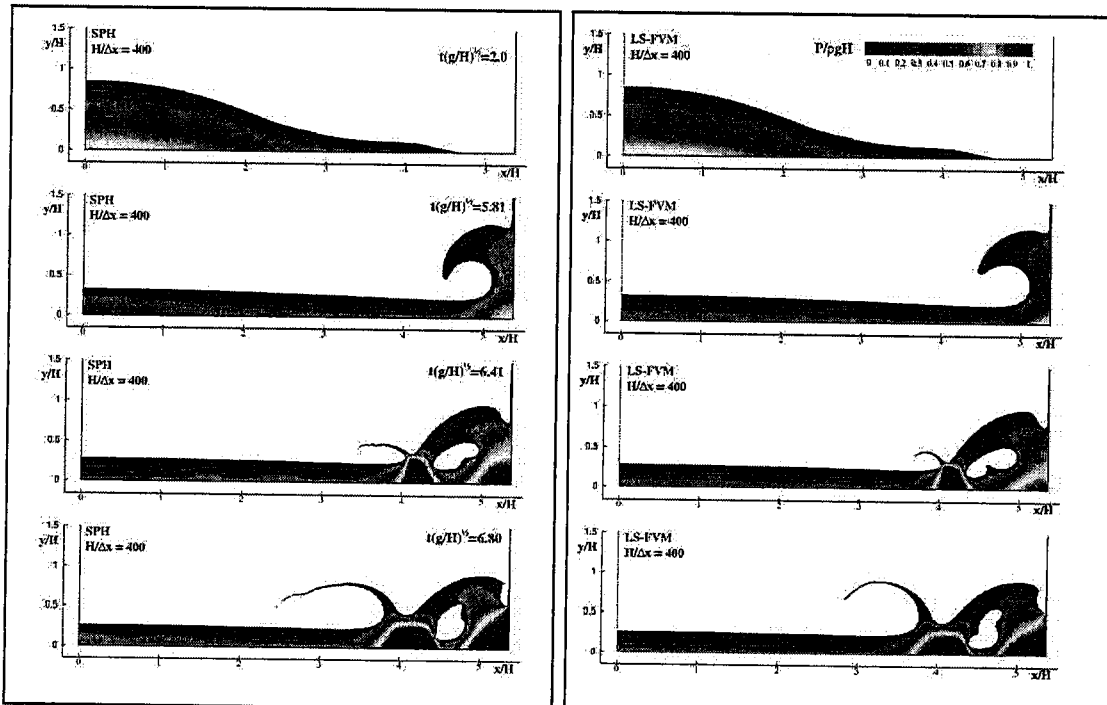


δ - SPH formulation

Comparison with standard SPH



δ - SPH formulation



Weakly-Compressible δ -SPH

Incompressible FVM

δ - SPH formulation

The δ -SPH maintains all the conservation properties of the standard SPH scheme

- ✓ Conservation of mass
- ✓ Conservation of linear and angular momenta
- ✓ If no viscosity, conservation of Energy (kinetic + potential + internal)

(see, for example, Antuono et al. 2015)

The dimensionless parameter δ varies in a narrow range of values (see Antuono et al. 2012) and **$\delta=0.1$ is a reliable choice in 2D simulations**

Green et al. (2019) have recently shown that δ – SPH formulation is similar to use Riemann Solver + MUSCL reconstruction in the Continuity equation to add diffusion

Incompressible SPH (ISPH)

Divergence-free incompressible SPH

ISPH methodology

- Solves incompressible Navier-Stokes equations

$$\frac{d\mathbf{u}}{dt} = -\frac{1}{\rho} \nabla P + \nu \nabla^2 \mathbf{u} + \mathbf{g} \quad \nabla \cdot \mathbf{u} = 0 \quad \frac{dm_i}{dt} = 0$$

- Incompressible SPH uses a **projection method** to enforce incompressibility by solving a Poisson equation for the pressure

$$\nabla \cdot \left(\frac{1}{\rho} \nabla P^{n+1} \right) = \frac{1}{\Delta t} \nabla \cdot \mathbf{u}^*$$

- No spurious pressure waves - pressure field is smooth and accurate when used with **particle regularisation or shifting**

(Xu et al JCP, 2009, 228; Lind et al., JCP, 2012, 231)

ISPH methodology

Gradients

$$\nabla P_i = \sum_j \frac{m_j}{\rho_j} (P_i - P_j) \nabla W_{ij}$$

Laplacian terms (i.e. Viscous forces)

$$\frac{1}{\rho_i} \nabla \cdot \mu_i \nabla \mathbf{u}_i = \frac{1}{\rho_i} \sum_j \frac{m_j}{\rho_j (x_{ij}^2 + \eta^2)} (\mu_i + \mu_j) \mathbf{x}_{ij} \cdot \nabla W_{ij} \mathbf{u}_{ij}$$

ISPH methodology

- The pressure Poisson equation

$$\nabla \cdot \left(\frac{1}{\rho} \nabla P^{n+1} \right) = \frac{1}{\Delta t} \nabla \cdot \mathbf{u}^*$$

- can be written in SPH formalism as

$$\sum_j \frac{m_j}{\rho_j (x_{ij}^2 + \eta^2)} \mathbf{x}_{ij} \cdot \nabla W_{ij} P_{ij} = \frac{1}{\Delta t} \sum_j \frac{m_j}{\rho_j} (\mathbf{u}_i^* - \mathbf{u}_j^*) \nabla W_{ij}$$

- which is of the form $\mathbf{A} \mathbf{X} = \mathbf{B}$ to be solved using Bi-CGSTAB solver

Incompressible SPH (ISPH)

Time integration

ISPH methodology

Enforce incompressibility using the projection method to ensure a divergence-free velocity field:

- Advect particles to an intermediate position \mathbf{x}^*

$$\mathbf{x}^* = \mathbf{x}^n + \mathbf{u}^n \Delta t$$

- Obtain an intermediate velocity \mathbf{u}^* based on the viscous and external forces

$$\mathbf{u}^* = \mathbf{u}^n + (\nu \nabla^2 \mathbf{u}^n + \mathbf{F}) \Delta t$$

- Solve the pressure Poisson equation to obtain Pressures at $n + 1$

$$\nabla \cdot \left(\frac{1}{\rho} \nabla P^{n+1} \right) = \frac{1}{\Delta t} \nabla \cdot \mathbf{u}^*$$

ISPH methodology

- Obtain the velocity at time $n + 1$ by projecting of \mathbf{u}^* onto divergent free space

$$\mathbf{u}^{n+1} = \mathbf{u}^* - \frac{1}{\rho} \nabla P^{n+1} \Delta t$$

- Advect particles to their positions at time $n + 1$

$$\mathbf{x}^{n+1} = \mathbf{x}^n + \left(\frac{\mathbf{u}^{n+1} + \mathbf{u}^n}{2} \right) \Delta t$$

Similar with WCSPH time we use a timestep based on the **CFL condition** which dictates the maximum timestep allowable

$$\Delta t = C_{cfl} \frac{\Delta x}{U_{\max}}$$

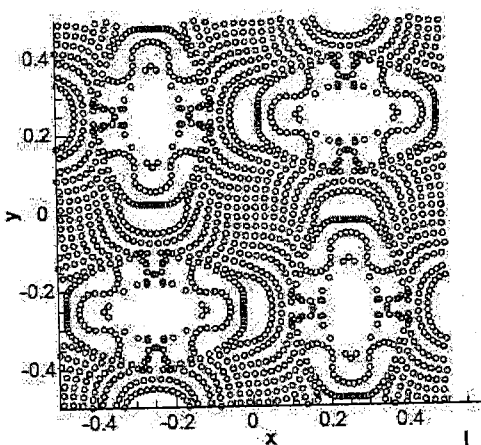
ISPH stability

- ISPH particles tend to follow the streamlines, which is great news for accuracy however,
- Stability suffers since,

$$\int_{\Omega} W(x - x', h) dx' \neq 1$$

$$\sum_j W_{ij} V_j \neq 1$$

due to particle clustering



Lind et al., 2012 (231), JCP

ISPH stability

- Use Fick's law of diffusion to move particles from regions of low concentration to high and vice versa,

$$J = -D \nabla C$$

or

$$\delta \mathbf{x}_i = -D \nabla C$$

with

$$\nabla C = \sum_j W_{ij} V_j$$

Final particle position

$$\mathbf{x}_i^{n+1} = \mathbf{x}_i^n + \delta \mathbf{x}_i$$

and D the diffusion coefficient:

$$D = Ah \|\mathbf{u}\| \Delta t$$

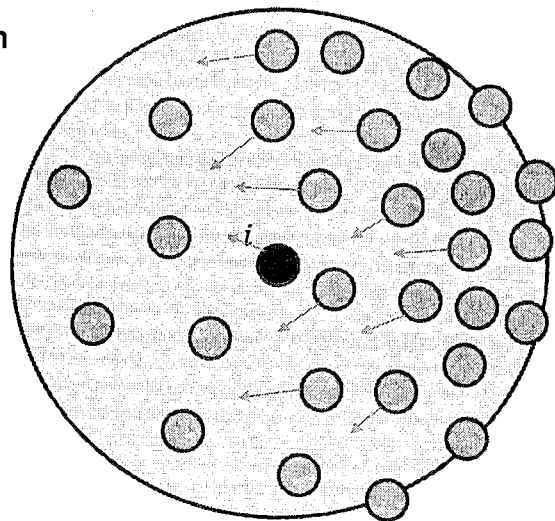
(Skillen et al., 2013)

$$D = Ah^2$$

(Lind et al., 2012 (231), JCP)

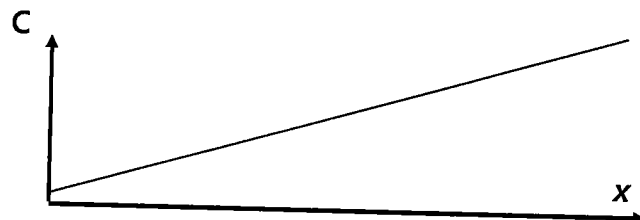
ISPH stability

Low
Concentration



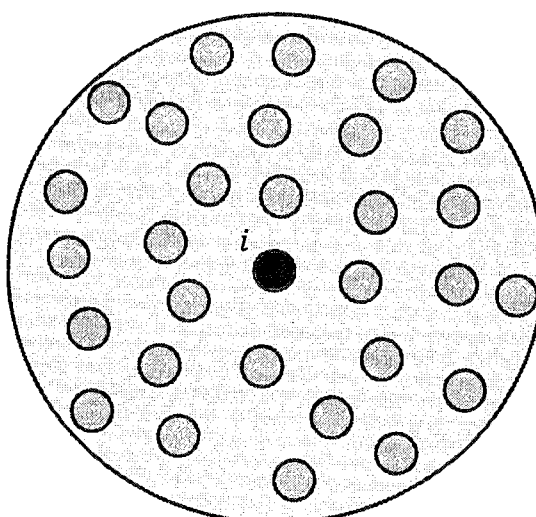
High
Concentration

$$\sum_j W_{ij} V_j \neq 1$$

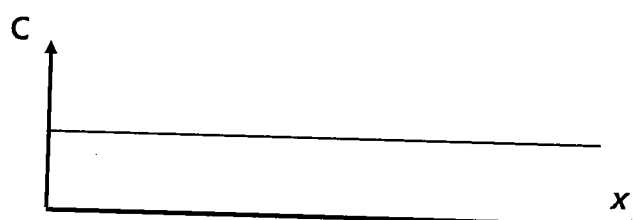


ISPH stability

Concentration
almost constant
throughout the
support of i

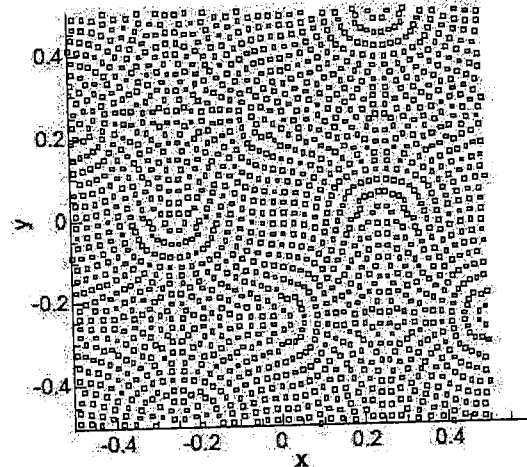
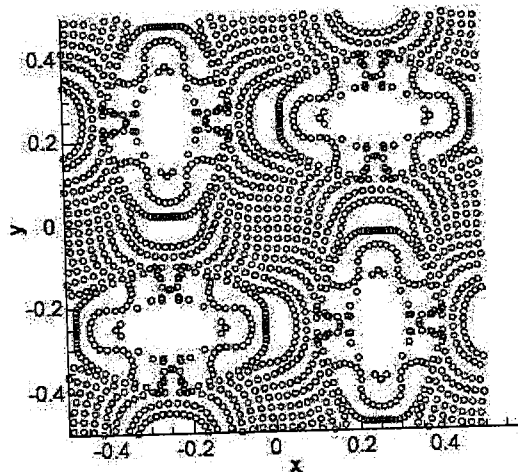


$$\sum_j W_{ij} V_j \approx 1$$



ISPH stability

- Taylor-Green vortices



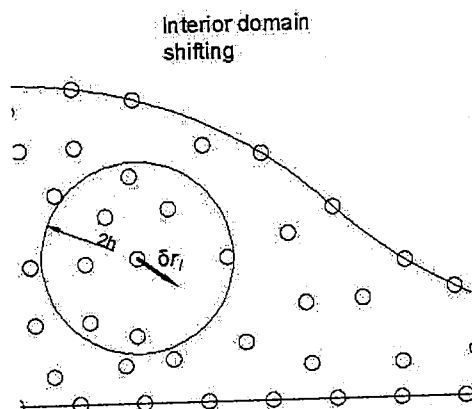
Lind et al., 2012 (231), JCP

ISPH stability

- Applicable to free-surface flows

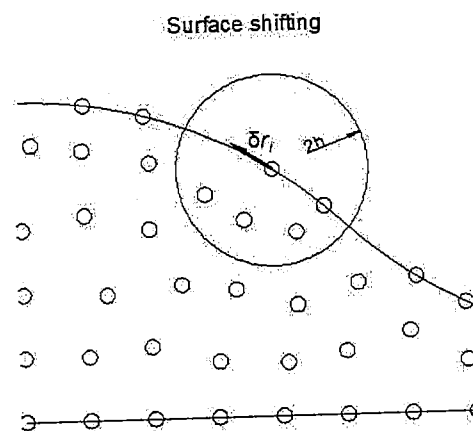
Interior fluid domain

$$\delta r_i^\alpha = -Ah^2 \frac{\partial C_i}{\partial x_i^\beta}$$



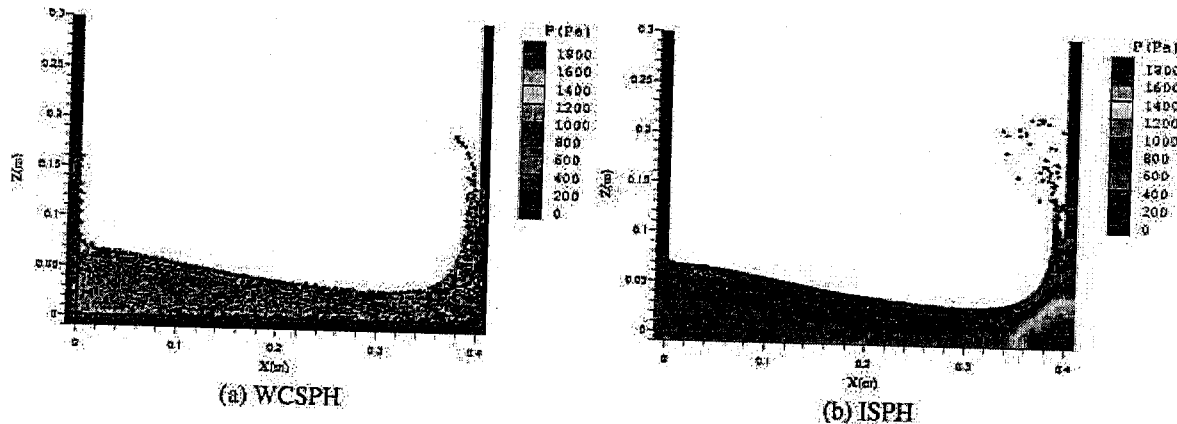
Free-surface domain

$$\delta r_i^\alpha = -Ah^2 \left(\frac{\partial C_i}{\partial s_i^\beta} s_i^\alpha \right)$$



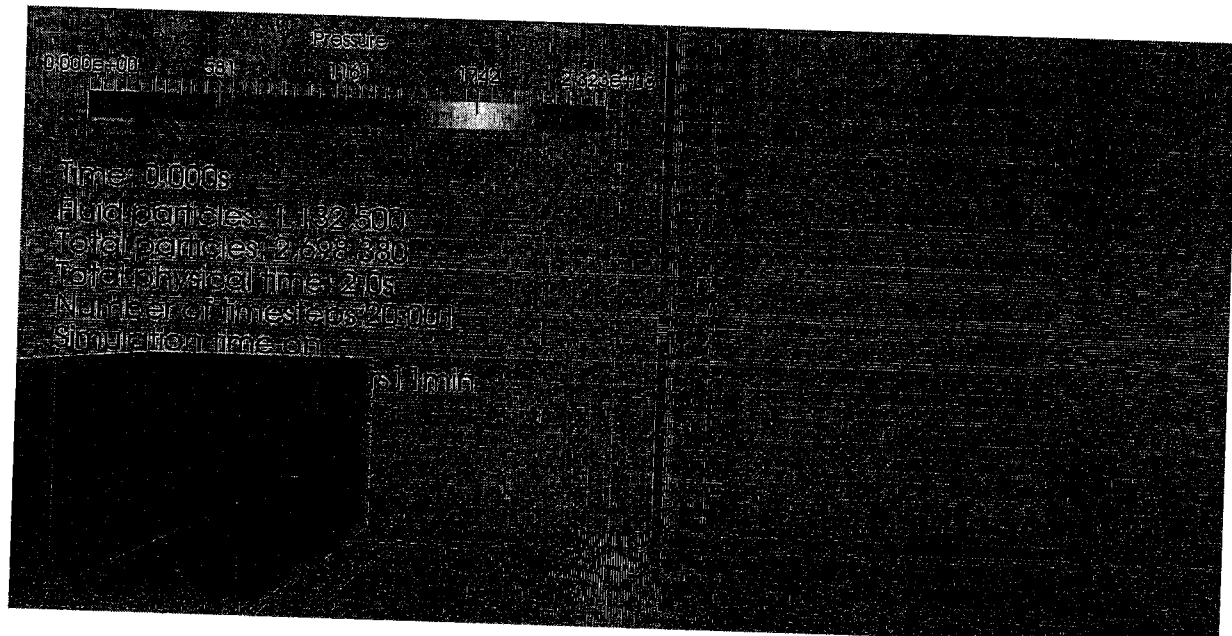
ISPH examples

Lee et al. (2008), JCP



ISPH examples

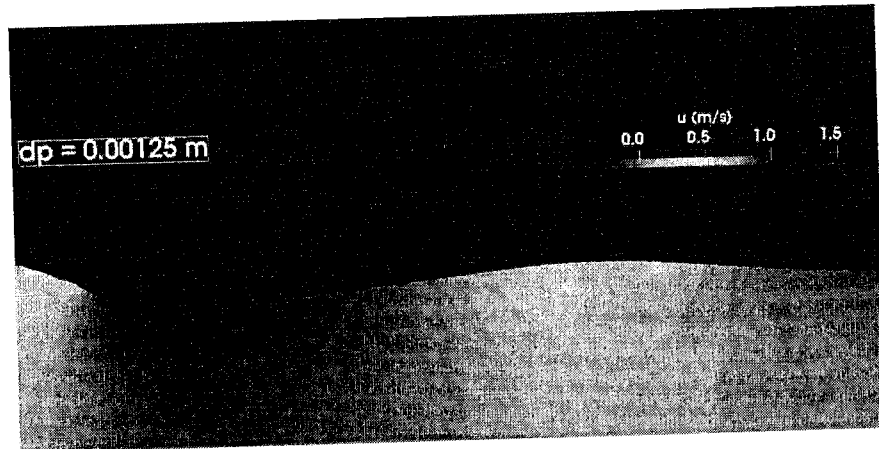
3D dambreak with column



Chow et al. (2018) C&F
Chow et al. (2019) CPC

ISPH examples

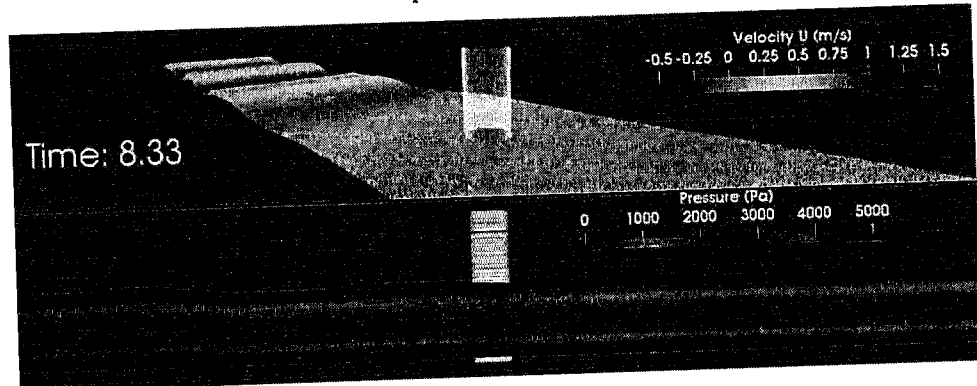
Plunging breaker



ISPH examples

Focussed wave group on cylinder
DHI experiments from Zang et al

F15 : H = 0.22 m, $f_p = 0.82$ Hz (Breaking)



Convergence tests on focussed waves

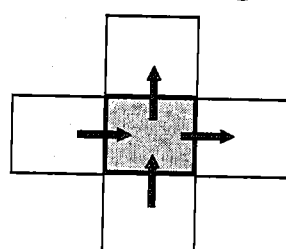
Chow et al. (2018) C&F
Chow et al. (2019) CPC

A quick recap on key SPH points 2

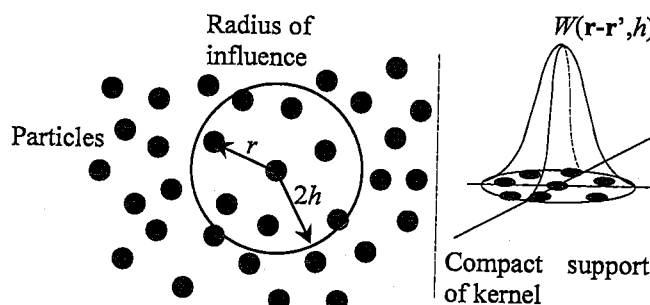
How does SPH compare in terms of computational expense? Consider:

Finite Volume (FVM) Stencil

4 neighbouring cells



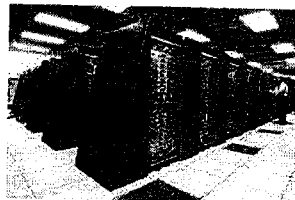
SPH Stencil



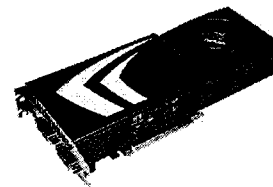
Real applications with millions of SPH particles can take a **long time** with so many neighbours (30 neighbours in 2-D, 100+ in 3-D)

Solution?

Use hardware acceleration



(i) Supercomputer (£millions!)



(ii) GPUs = graphics cards in all devices (£300 - £3000)

What SPH can & cannot do

- **Very general method:** number of potential applications is broad
- **Violent free-surface motion** is implicitly captured
- Essentially, **complex geometries** do not present a problem
- But, without hardware acceleration, SPH can take a **long time**
- So, very large domains (with 10^{10} particles) are not feasible
- Hence, very good for providing **finer level of detail** to couple/feed to other models

SPHERIC

International SPH Initiative: <http://spheric-sph.org>

HOME SPHERIC GOVERNANCE EVENTS AND ACTIVITIES GRAND CHALLENGES VALIDATION TESTS SPH SOFTWARE SPH PROJECTS SPH JOBS SPH LITERATURE

Welcome to SPHERIC

SPHERIC is the International organisation representing the community of researchers and industrial users of Smoothed Particle Hydrodynamics (SPH).



spheric
ERCOFTAC

- Founding member
- Steering Committee
- Webmaster (2005-2015)
- Chair (2015 - 2020)
 - 11 International Workshops
 - 2015 in Parma**
 - Training Day
- 75 Institutions are members: universities, government research labs & 47 industrial companies

As a purely Lagrangian technique, SPH enables the simulation of highly distorting fluids and solids. Fields including free-surface flows, solid mechanics, multi-phase, fluid-structure interaction and astrophysics, where Eulerian methods can be difficult to apply represent ideal applications of this meshless method.

History

The SPH method was developed to study non-axisymmetric phenomena in astrophysics in the 1970s, but its application to engineering emerged in the 1990s and early 2000s. In the past twenty years the method has developed rapidly in many fields of application from impacts to fracture to breaking waves and fluid-structure interaction.

Following the impulse generated by a collection of local initiatives in 2005 (France, UK, Italy...), a need to foster and collaborate efforts and

The current state of SPH

- Research into SPH is now in full swing:
 - Every aspect is being thoroughly investigated: Turbulence, Boundary conditions
 - Mathematical foundations are being secured
 - Multi-phase & multi-scale
 - “Supercharging” = making the method feasible computationally
 - Applied to harder and harder problems
- SPHERIC has given a much needed step change in quality
- Rather than being a toy method, it is being properly considered by industry
- Hardware acceleration is still immature
- Coupling is underway

SPH Applications: Examples

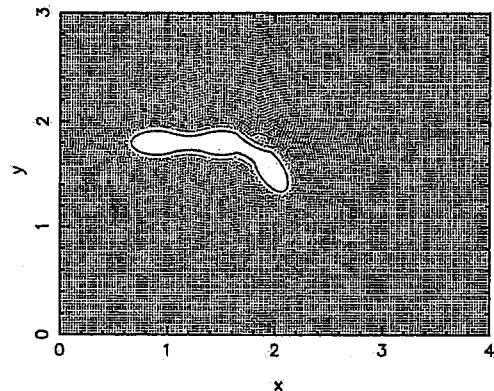
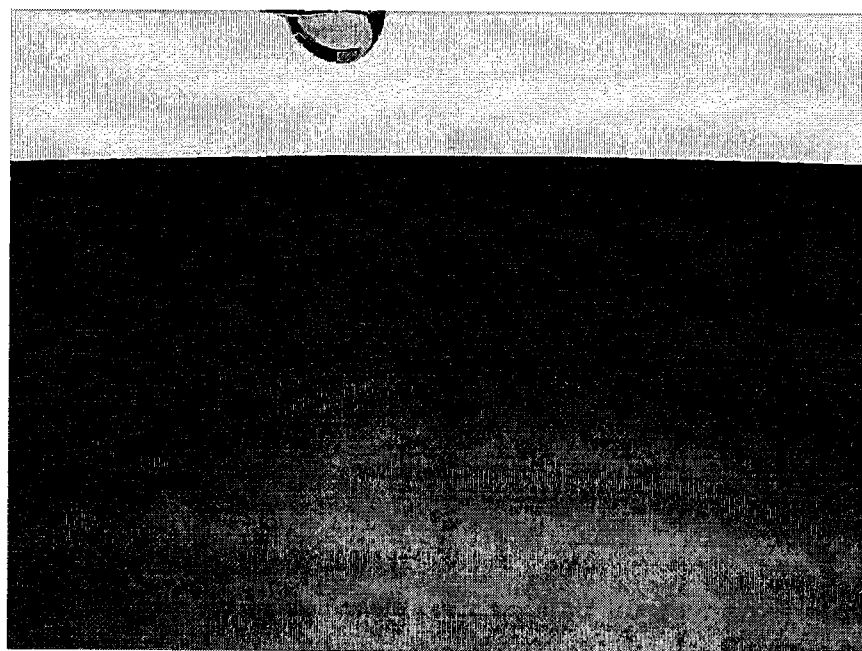


Fig. 3. Initial position of the linked bodies with skin after a period of damping.

Swimming Fish (Kajtar & Monaghan 2008)

149

SPH Applications: Examples



Water Glass (Premoze et al. 2003, University of Utah)

150

SPH Applications: Examples



Flooding Corridor (Premoze et al. 2003, University of Utah)

151

SPH in Hollywood

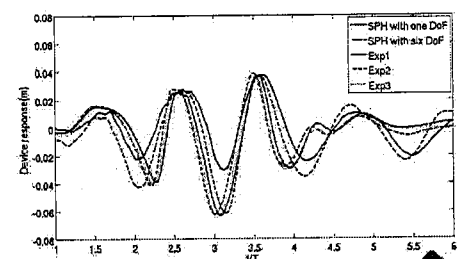
- You've seen SPH before

Classic Example:

Gollum falling into Lava



Validate with Experimental Data or
Analytical Solution?

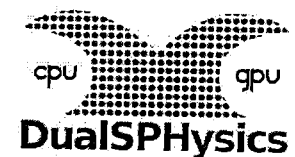
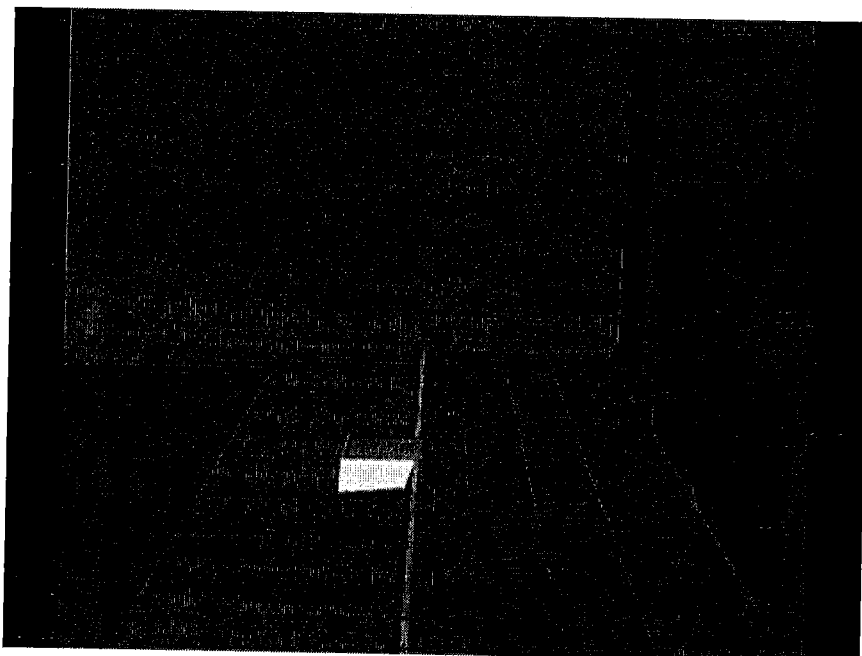


Scientific Validation is crucial to
all our work for engineering

152

The Future: (Multi) Hybrid Chips

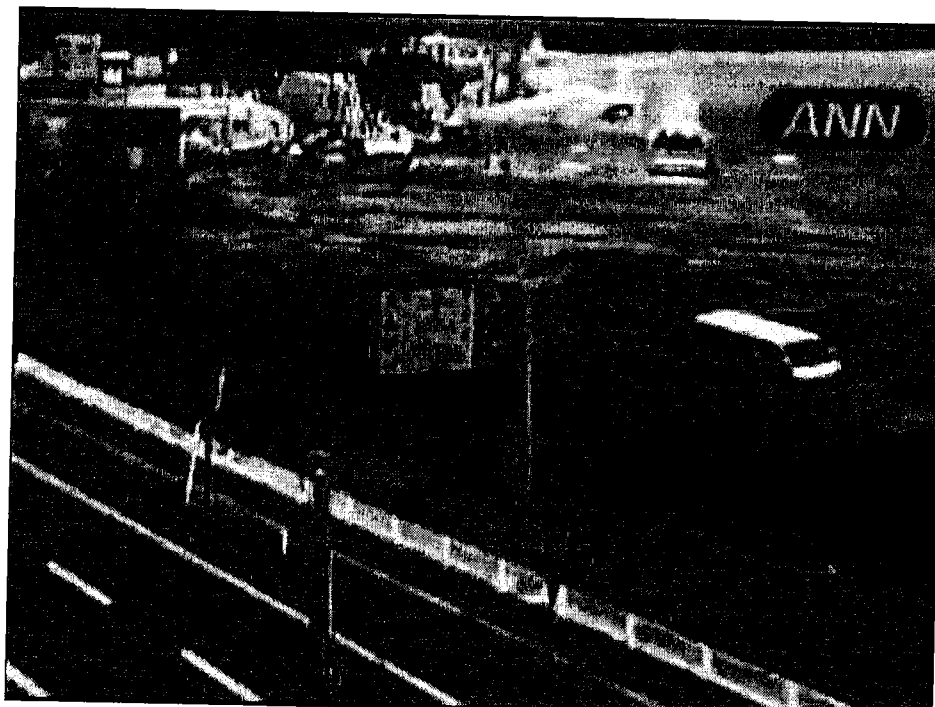
- Dual-SPHysics (cpu & GPU)
- Crespo et al.



153

Real-World Applications: Example

2011 Japanese Tsunami



154

Real-World Applications: Example



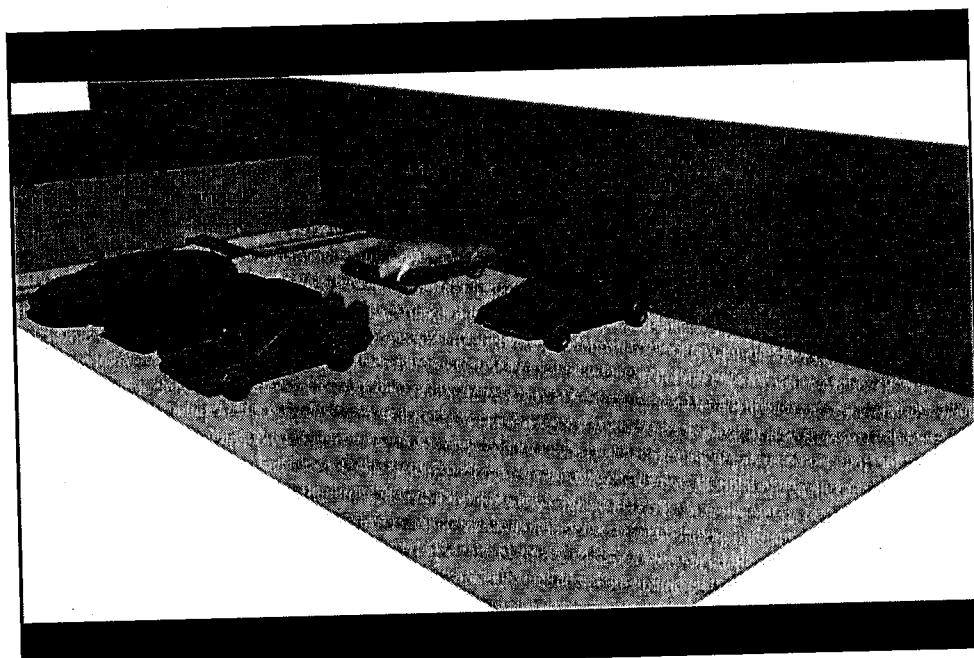
Wave Generated by Vajont Rockslide

(Vacondio et al. Advances in Water resources 2013)

155

Particles AND Rigid Bodies

2011 Japanese Tsunami



cpu gpu
DualSPHysics

156

References

- Gingold, R.A.; Monaghan, J.J., Smoothed particle hydrodynamics - Theory and application to non-spherical stars, *Monthly Notices of the Royal Astronomical Society*, vol. 181, Nov. 1977, p. 375-389.
- Lucy, L. B., A numerical approach to the testing of the fission hypothesis, *Astronomical Journal*, vol. 82, Dec. 1977, p. 1013-1024.
- Quinlan, N.J., Basa, M., Lastiwka, M., Truncation error in mesh-free particle methods, *International journal for numerical methods in engineering*, vol. 66 (13), 2006, p. 2064-2085.
- J. Bonet, J., Lok, T.-S.L., Variational and momentum preservation aspects of Smooth Particle Hydrodynamic formulations, *Computer Methods in Applied Mechanics and Engineering*, vol. 180, 1999, p. 97-115.
- Chen, J.K., Beraun, J.E., Jih, C.J., Completeness of corrective smoothed particle method for linear elastodynamics, *Computational Mechanics*, vol. 24, 1999, p. 273-285.
- Dilts, G. A., Moving-least-squares-particle hydrodynamics—I. Consistency and stability. *Int. J. Numer. Meth. Engng.*, vol. 44, 1999, p. 1115-1155.
- Liu, M.B., Liu, G.R., Restoring particle consistency in smoothed particle hydrodynamics, *Applied Numerical Mathematics*, vol. 56, 2006, p. 19-36.
- Morris, J.P., Fox, P.J., Zhu, Y., Modeling Low Reynolds Number Incompressible Flows Using SPH, *Journal of Computational Physics*, vol. 136, 1997, p. 214-226.
- Monaghan, J.J., An introduction to SPH, *Computer Physics Communications*, vol. 48, 1989, p. 89-96.

157

- Monaghan, J.J., Simulating free surface flows with SPH, *Journal of Computational Physics*, vol. 110 1994, p. 399-406.
- Monaghan, J.J., Smoothed particle hydrodynamics, *Annual review of Astronomy and Astrophysics*, vol. 30, 1992, p. 543-574.
- Monaghan, J.J., Kos, A., Issa N., Fluid motion generated by impact. *Journal of waterway, port, coastal and ocean engineering*, vol. 129, 2003, p. 250-259
- Monaghan, J.J., Smoothed particle hydrodynamics, *Reports on Progress in Physics*, 68, 2005, p. 1703-1759.
- Kajtar, J., Monaghan,J.J., SPH simulations of swimming linked bodies, *Journal of Computational Physics*, vol. 227, 2008, p. 8568-8587,
- Violeau, D. Issa R., Numerical modelling of complex turbulent free-surface flows with the SPH method: an overview, *International Journal for Numerical Methods in Fluids*, vol. 53, 2007, p. 277 – 304
- Tafuni, A., Domínguez, J.M., Vacondio, R., Crespo A.J.C., A versatile algorithm for the treatment of open boundary conditions in smoothed particle hydrodynamics gpu models, *Computer Methods in Applied Mechanics and Engineering*, vol. 342, 2018, p. 604-624
- Molteni, D., Colagrossi, A., A simple procedure to improve the pressure evaluation in hydrodynamic context using the SPH, *Computer Physics Communications*, vol. 180, 2009, p. 861-872.

158

- Ferrari, A., Dumbser, M., Toro, E.F., Armanini, A., A new 3D parallel SPH scheme for free surface flows, *Computers & Fluids*, vol. 38, 2009, p. 1203-1217.
- Antuono, M., Colagrossi, A., Marrone, S., Molteni, D., Free-surface flows solved by means of SPH schemes with numerical diffusive terms, *Computer Physics Communications*, vol. 181, 2010, p. 532-549.
- Antuono, M., Marrone, S., Colagrossi, A., Bouscasse, B., Energy balance in the δ -SPH scheme, *Computer Methods in Applied Mechanics and Engineering*, vol. 289, 2015, p. 209-226.
- Green, M.D., Vacondio, R., Peiró, J. A smoothed particle hydrodynamics numerical scheme with a consistent diffusion term for the continuity equation, *Computers & Fluids*, vol. 179, 2019, p. 632-644.
- Xu, R., Stansby, P.K., Laurence, D., Accuracy and stability in incompressible SPH (ISPH) based on the projection method and a new approach, *Journal of Computational Physics*, vol. 228, 2009, p. 6703-6725.
- Lind, S.J., R. Xu, P.K. Stansby, B.D. Rogers, Incompressible smoothed particle hydrodynamics for free-surface flows: A generalised diffusion-based algorithm for stability and validations for impulsive flows and propagating waves, *Journal of Computational Physics*, vol. 231, 2012, p. 1499-1523.
- Skillen, A. Lind, S.J., Stansby, P.K., Rogers, B.D., Incompressible smoothed particle hydrodynamics (SPH) with reduced temporal noise and generalised Fickian smoothing applied to body–water slam and efficient wave–body interaction, *Computer Methods in Applied Mechanics and Engineering*, vol. 265, 2013, p. 163-173.

159

- Vacondio, R., Mignosa, P., Pagani, S., 3D SPH numerical simulation of the wave generated by the Vajont rockslide, *Advances in Water Resources*, vol. 59, 2013, p. 146-156,
- Chow AD, Rogers BD, Lind SJ, Stansky PK, Numerical wave basin using incompressible smoothed particle hydrodynamics (ISPH) on a single GPU with vertical cylinder test cases, *Computers & Fluids*, vol. 179, 2019, p. 543-562
- Chow A.D., Rogers B.D., Lind S.J., Stansby P.K., Incompressible SPH (ISPH) with fast Poisson solver on a GPU, *Computer Physics Communications*, vol. 226, 2018, p. 81-103
- Lee, E-S., Moulinec, C., Xu, R., Violeau, D., Laurence, D., Stansby, P.K., Comparisons of weakly compressible and truly incompressible algorithms for the SPH mesh free particle method, *Journal of Computational Physics*, vol. 227, 2008, p. 8417-8436.

160